

Safe Flow Matching: Robot Motion Planning with Control Barrier Functions

Xiaobing Dai*
TUM

Zewen Yang*[†]
TUM

Dian Yu*
TUM

Shanshan Zhang
UPC

Hamid Sadeghian
TUM

Sami Haddadin
MBZUAI

Sandra Hirche
TUM

Abstract: Recent advances in generative modeling have led to promising results in robot motion planning, particularly through diffusion and flow matching (FM)-based models that capture complex, multimodal trajectory distributions. However, these methods are typically trained offline and remain limited when faced with new environments with constraints, often lacking explicit mechanisms to ensure safety during deployment. In this work, we propose Safe Flow Matching (SafeFlow), a motion planning framework, for trajectory generation that integrates flow matching with safety guarantees. SafeFlow leverages our proposed flow matching barrier functions (FMBF) to ensure the planned trajectories remain within safe regions across the entire planning horizon. Crucially, our approach enables training-free, real-time safety enforcement at test time, eliminating the need for retraining. We evaluate SafeFlow on a diverse set of tasks, including planar robot navigation and 7-DoF manipulation, demonstrating superior safety and planning performance compared to state-of-the-art generative planners. Comprehensive resources are available on the project website: <https://safeflowmatching.github.io>

Keywords: Flow Matching, Safe Motion Planning, Control Barrier Functions, Trajectory Generation

1 Introduction

Enabling robots to autonomously generate safe and feasible motions in dynamic environments remains one of the central challenges in robotic learning and motion planning. Recent advances in deep generative modeling, particularly in diffusion models, have significantly expanded the capabilities of robots to learn diverse and high-dimensional behaviors from demonstrations or interactions. These models have proven effective in modeling multimodal trajectory distributions, enabling robots to adaptively generate context-dependent motions across various tasks, such as navigation [1], object manipulation [2], and locomotion [3]. Despite their success, diffusion models come with notable limitations. Specifically, the inference process is typically slow and computationally intensive,

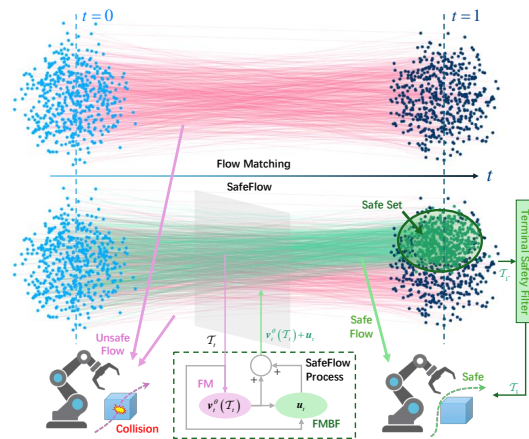


Figure 1: SafeFlow process illustration.

*Equal contribution.

[†]Corresponding author. Email: zewen.yang@tum.de.

as it involves iteratively solving a stochastic differential equation over many denoising steps [4]. Furthermore, while diffusion models can be conditioned on goals or task descriptions, they generally lack formal safety guarantees, which is crucial when deploying robots in dynamic environments with obstacles, humans, or other agents. Recent works have begun to address these concerns by incorporating safety constraints into diffusion-based frameworks (e.g., via model predictive control [5] or barrier functions [6]), but such repeated inference using diffusion models further increases computational complexity and may compromise inference quality or task performance.

To overcome these challenges, we turn to Flow Matching (FM)—a recently emerging generative modeling framework that offers a promising alternative to diffusion models [7]. Instead of relying on stochastic processes, FM defines a deterministic flow field—governed by an ordinary differential equation—that smoothly transforms samples from a simple prior distribution into target data samples [8]. More importantly, the FM framework is amenable to explicit constraint integration, making it a natural candidate for generating safe robot motions [9, 10] (as shown in Fig. 1).

In this work, we introduce safe flow matching (SafeFlow), a novel method for constraint-aware motion planning that combines the efficiency and flexibility of FM with the formal safety guarantees provided by flow matching barrier functions (FMBFs), inspired by control barrier functions (CBFs). SafeFlow learns a continuous-time vector field that maps random waypoints from a prior distribution to goal-directed robot trajectories, while simultaneously ensuring that the generated trajectories respect safety constraints. By leveraging finite-time flow invariance principles [7], we embed a regularization term directly into the FM model, enabling real-time generation of safe and feasible motions without sacrificing generation quality or expressiveness. We compare SafeFlow to state-of-the-art (SOTA) methods, demonstrating the superiority of our method across six performance metrics, e.g., safety, smoothness, and efficiency. The main contributions of this paper are:

- SafeFlow, a novel FM framework for robot motion planning under safety constraints.
- A theoretically grounded integration of control barrier functions, as a plug-and-play safety module, into flow-based generative models to ensure safe trajectory generation.
- Empirical demonstrations on the superior safety capabilities and planning performance of SafeFlow across multiple tasks.

2 Related Work

Generative models for robot learning have gained considerable attention in recent years. This section reviews recent advancements in diffusion-based and flow-based methods, with a focus on their applications to robot learning.

Diffusion-based Models for Robot Learning. Diffusion models have been effectively utilized in various robot learning domains, including motion planning, imitation learning, and reinforcement learning, as demonstrated by works such as [2, 3, 11]. Especially in imitation learning, diffusion models have been leveraged to produce robot trajectories based on expert demonstrations. For example, Pearce et al. [12] and Reuss et al. [13] employ diffusion models to develop policies that replicate expert behaviors. Additionally, Xian et al. [14] introduces ChainedDiffuser, a novel policy architecture that integrates action keypose prediction with trajectory diffusion generation for robotic manipulation tasks. To tackle long-horizon planning and task execution, Li et al. [15] and Mishra et al. [16] propose skill-centric diffusion models that combine learned distributions to create extended plans during inference. For generating control actions, Chi et al. [17] presents Diffusion Policy, which frames policy learning as a conditional denoising diffusion process over the robot’s action space, conditioned on 2D observation features. This concept is advanced by Ze et al. [18] in their 3D Diffusion Policy, which incorporates complex 3D visual representations to enable generalizable visuomotor policies from just a few dozen expert demonstrations.

Recent efforts have also aimed to ensure that generated trajectories comply with the physical laws governing robot dynamics. For instance, Gadginmath and Pasqualetti [3] embed system dynamics directly into the denoising process, while Chen et al. [19] use generated state sequences with

an inverse dynamics model to derive actions for coordinated bimanual tasks. To enforce safety and dynamical constraints, Li et al. [20] incorporate penalties for constraint violations into the loss function, though this method does not guarantee strict adherence to hard constraints. Alternatively, Bouvier et al. [21] project generated policies onto a dynamically admissible manifold during training and inference. However, this technique underapproximates the reachable set using a polytope, relying on the assumption of smooth nonlinear dynamics and environments. Drawing inspiration from CBFs, Xiao et al. [22], Mizuta and Leung [23] propose SafeDiffuser and CoBL, frameworks aimed at enforcing safety constraints within reverse diffusion models for safe planning. However, a critical limitation remains: as acknowledged by the authors, CBFs rely on the assumption that the initial state of the reverse diffusion process lies within the safe set, an assumption that is fundamentally violated, since the initial state is sampled from pure noise. Furthermore, due to the probabilistic nature of diffusion models, there is no guarantee that the generated trajectories will remain within the safe set throughout the process. In addition, the manipulation tasks considered in [22] are overly simplistic, addressing only joint limit constraints while overlooking critical factors such as collision avoidance. As a result, the practical applicability of this framework to real-world robot learning and control remains limited.

Flow-based Models for Robot Learning. Flow matching models have emerged as a promising alternative to diffusion models, offering potential improvements in efficiency and performance for robotic applications. For instance, Zhang and Gienger [24] introduces a flow matching policy that utilizes affordance-based reasoning for manipulation tasks. Departing from image-based inputs, Chisari et al. [25] employs point clouds with conditional flow matching to generate robot actions. To enhance efficiency, Zhang et al. [26] proposes a flow policy that uses consistency flow matching with a straight-line flow, enabling one-step generation and striking a balance between speed and effectiveness. However, limitations persist in complex manipulation scenarios. Capitalizing on the strengths of flow matching, Braun et al. [27] applies these models to robot states defined on a Riemannian manifold. This approach better captures high-dimensional multimodal distributions, improving the handling of complex robotic systems.

3 Preliminaries

3.1 Flow Matching Model

In this paper, we intend to generate the motion trajectory $\mathcal{T}(\cdot) : [0, 1] \rightarrow \mathbb{R}^{(H+1) \times d_s}$ of robotics with a horizon $H \in \mathbb{N}_{>0}$, which is represented as a sequence of states $\mathbf{s}_t^k \in \mathbb{S} \subseteq \mathbb{R}^{d_s}$ for $t \in [0, 1]$ and $k = 0, \dots, H$, i.e., $\mathcal{T}_t = \mathcal{T}(t) = [(\mathbf{s}_t^0)^\top, \dots, (\mathbf{s}_t^H)^\top]^\top \in \mathbb{S}^{H+1} \subseteq \mathbb{R}^{(H+1)d_s}$ with the dimension $d_s \in \mathbb{N}_{>0}$ and $d = d_s(H + 1)$. To this end, a flow matching model is defined through an ODE governed by a time-dependent vector field $\mathbf{v}^\theta : [0, 1] \times \mathbb{R}^d \rightarrow \mathbb{R}^d$ parameterized by a neural network with parameters θ , which induces a time-dependent flow map $\psi(\cdot, \cdot) : [0, 1] \times \mathbb{R}^d \rightarrow \mathbb{R}^d$ with $d \in \mathbb{N}_{>0}$ [7]. Specifically, the flow matching model is written as

$$\frac{d}{dt} \psi_t(\boldsymbol{\tau}) = \mathbf{v}_t^\theta(\psi_t(\boldsymbol{\tau})), \quad (1)$$

where $\psi_t(\boldsymbol{\tau}) := \psi(t, \boldsymbol{\tau})$ and $\mathbf{v}_t^\theta := \mathbf{v}(t, \boldsymbol{\tau})$ with initial conditions $\psi_0(\boldsymbol{\tau}_0) = \boldsymbol{\tau}_0$. Considering a start $\mathcal{T}_0 = \boldsymbol{\tau}_0$ at $t = 0$, the vector field generates the probability path p_t if its flow $\psi_t(\boldsymbol{\tau})$ satisfies

$$\mathcal{T}_t := \psi_t(\mathcal{T}_0) \sim p_t \quad \text{for} \quad \mathcal{T}_0 \sim p_0 \quad (2)$$

Thus, the velocity field \mathbf{v}_t^θ enables sampling from the probability path p_t by solving the ODE. The objective of flow matching is to train a parameterized vector field \mathbf{v}_t^θ such that its induced flow ψ_t generates a probability path p_t , transitioning from an initial distribution $p_0 = p$ to the target data distribution $p_1 = q$.

3.2 Safe Invariance in Dynamical Systems

To ensure the safety of the generated trajectory \mathcal{T} , CBFs are introduced here. In particular, consider a control-affine system

$$\dot{\mathbf{x}}_t = \mathbf{f}(\mathbf{x}_t) + \mathbf{g}(\mathbf{x}_t)\mathbf{u}_t, \quad (3)$$

where $\mathbf{x}_t \in \mathbb{X} \subset \mathbb{R}^n$, $\mathbf{f}(\cdot) : \mathbb{X} \rightarrow \mathbb{R}^n$ and $\mathbf{g}(\cdot) : \mathbb{X} \rightarrow \mathbb{R}^{n \times m}$ are locally Lipschitz, and $\mathbf{u}_t \in \mathbb{R}^m$ is the control input for all time t . Moreover, a super level set $\mathbb{C} := \{\mathbf{x}_t \in \mathbb{R}^n | h(\mathbf{x}_t) \geq 0\}$ is defined via a continuously differentiable equation $h(\cdot) : \mathbb{X} \rightarrow \mathbb{R}$, which encodes safety guarantees for Eq. (3).

Definition 1 ([6]). *Given a safe set \mathbb{C} , $h(\mathbf{x})$ is a time-invariant CBF for system Eq. (3) if there exists a class \mathcal{K} function $\alpha(\cdot)$ such that for all $t \in \mathbb{R}_{0,+}$ it has $\mathbf{x}_0 \in \mathbb{C}$ and*

$$\sup_{\mathbf{u} \in \mathbb{R}^m} \{L_{\mathbf{f}}h(\mathbf{x}_t) + L_{\mathbf{g}}h(\mathbf{x}_t)\mathbf{u} + \alpha(h(\mathbf{x}_t))\} \geq 0, \quad (4)$$

where $L_{\mathbf{f}}h(\mathbf{x}_t)$, $L_{\mathbf{g}}h(\mathbf{x}_t)$ denote the Lie derivatives of $h(\mathbf{x}_t)$ along $\mathbf{f}(\mathbf{x}_t)$ and $\mathbf{g}(\mathbf{x}_t)$, respectively.

Notably, the initial safety condition $\mathbf{x}_0 \in \mathbb{C}$ is generally not satisfied in the reverse diffusion process, which has been overlooked in previous works [22, 23]. Thankfully, the task of driving the system Eq. (3) into the safe set during the reverse diffusion process can be defined as prescribed-time safety as follows.

Definition 2 ([28]). *A system in Eq. (3) is prescribed-time safe with a predefined time $T_d \in \mathbb{R}_{>0}$, if $\mathbf{x}_t \in \mathbb{C}$ for any $t \geq T_d$ with arbitrary $\mathbf{x}_0 \in \mathbb{X}$.*

To ensure safety in FM, we draw inspiration from the safety guarantees provided by CBFs and propose an adaptation for trajectory generation. The mathematical formulation of this approach is presented in the following section.

4 Safe Flow Matching

The objective is to generate a trajectory $\mathcal{T} = [(s^0)^\top, \dots, (s^H)^\top]^\top$ that closely aligns with a target distribution while remaining within a predefined safe set. In this section, we formally define safe flow matching and introduce the concept of flow matching barrier functions (FMBFs). Furthermore, we propose safety regularization terms designed to enforce compliance with safety constraints during trajectory generation.

4.1 Safe Flow Matching under Unified Constraints

In this subsection, we consider a safe set $\mathbb{C}_s \subseteq \mathbb{S}$ defined for each state \mathbf{s}^i , $i = 0, \dots, H$, characterized by a single continuous function $h(\cdot) : \mathbb{S} \rightarrow \mathbb{R}$. Then the generated trajectory \mathcal{T} is called safe if all generated states \mathbf{s}^i remain in the safe set \mathbb{C}_s , which is mathematically defined as follows.

Definition 3 (Trajectory Safety). *A trajectory \mathcal{T} with length $H + 1$ is safe w.r.t $h(\cdot)$, if*

$$h(\mathbf{E}_i \mathcal{T}) \geq 0, \quad \forall i \in \{0, 1, \dots, H\}, \quad (5)$$

where $\mathbf{E}_i \in \mathbb{R}^{d_s \times d}$ is a selection matrix defined as $\mathbf{E}_i = [\mathbf{0}_{d_s \times i d_s}, \mathbf{I}_{d_s}, \mathbf{0}_{d_s \times (H-i)d_s}]$.

Accordingly, we introduce the definition of safe flow matching trajectory generation as follows.

Definition 4 (Safe Flow Matching). *A flow matching process is called safe if the generated trajectory \mathcal{T}_1 at $t = 1$ satisfies the safety conditions in Definition 3 for any initial sample $\mathcal{T}_0 \sim p_0$.*

To ensure the safety of the generated trajectory as in Definition 4, we consider the control input $\mathbf{u}_t = [\mathbf{u}_t^0, \dots, \mathbf{u}_t^H]^\top$ serving as a regularization term to steer the flow toward a safe manifold, where $\mathbf{u}_t^i \in \mathbb{R}^{d_s}$ with $i = 1, \dots, H$. Therefore, the flow model is formulated as

$$\frac{d}{dt} \psi_t(\boldsymbol{\tau}) = \mathbf{v}_t^\theta(\boldsymbol{\tau}) + \mathbf{u}_t, \quad \forall t \in [0, 1]. \quad (6)$$

Drawing inspiration from CBFs, we propose an FMBF to enforce safety constraints in the flow matching framework, which is defined as follows.

Definition 5 (Flow Matching Barrier Function). A function $h(\cdot)$ is called a flow matching barrier function (FMBF) if it satisfies the following conditions:

1. For all $i = 0, \dots, H$ and $t \in [0, 1)$, it has

$$\sup_{\mathbf{u}_t^i \in \mathbb{R}^{d_s}} \left\{ \frac{dh(\mathbf{E}_i \mathcal{T}_t)}{d\mathbf{E}_i \mathcal{T}_t} \mathbf{E}_i \mathbf{v}_t^\theta(\boldsymbol{\tau}) + \frac{dh(\mathbf{E}_i \mathcal{T}_t)}{d\mathbf{E}_i \mathcal{T}_t} \mathbf{u}_t^i + \varphi(t, h(\mathbf{E}_i \mathcal{T}_t)) h(\mathbf{E}_i \mathcal{T}_t) \right\} \geq 0, \quad (7)$$

with $\varphi(t, h(\mathbf{s})) = \varphi_0 \in \mathbb{R}_{>0}$ if $h(\mathbf{s}) \geq 0$, and $\varphi(t, h(\mathbf{s})) = \varphi_1(t)$, otherwise, where $\varphi_1(\cdot) : [0, 1) \rightarrow \mathbb{R}_{>0}$ monotonically increases satisfying $\lim_{t \rightarrow 1^-} \varphi_1(t) = \infty$ and $\int_0^{1^-} \varphi_1(s) ds = \infty$.

2. For all $i = 0, \dots, H$, the terminal condition holds: $h(\mathbf{E}_i \mathcal{T}_1) \geq 0$.

Build upon the FMBF, the safety guarantee is derived in the following theorem³.

Theorem 1. Suppose $h(\cdot)$ is a valid FMBF as per Definition 5. Then, the FM process is safe according to Definition 4, ensuring that the generated trajectory \mathcal{T}_1 satisfies the safety condition in Definition 3.

Although valid FMBFs ensure safety for both the trajectory and the FM process, the selection of an appropriate regularization term \mathbf{u}_t for each $t \in [0, 1)$ remains a critical challenge. To minimize the influence of \mathbf{u}_t on the distribution's alignment with the target p_1 , the regularization term should be kept as small as possible in magnitude. To this end, we determine \mathbf{u}_t by solving the following optimization problem:

$$\mathbf{u}_t = \arg \min_{\mathbf{u} = [\mathbf{u}^0 \top, \dots, \mathbf{u}^H \top] \top \in \mathbb{R}^d} \|\mathbf{u}\|^2 \quad (8a)$$

$$\text{s.t. } \frac{\partial h(\mathbf{E}_i \mathcal{T}_t)}{\partial \mathbf{E}_i \mathcal{T}_t} \mathbf{E}_i \mathbf{v}_t^\theta(\boldsymbol{\tau}) + \frac{\partial h(\mathbf{E}_i \mathcal{T}_t)}{\partial \mathbf{E}_i \mathcal{T}_t} \mathbf{u}_t^i + \varphi(t, h(\mathbf{E}_i \mathcal{T}_t)) h(\mathbf{E}_i \mathcal{T}_t) \geq 0, \quad \forall i \in \{0, \dots, H\}, \quad (8b)$$

which can be considered as a quadratic programming (QP) problem due to the quadratic objective function and linear constraint w.r.t \mathbf{u}_t . The explicit closed-form expression of \mathbf{u}_t refers to Appendix B.

4.2 Safe Flow Matching under Composite Constraints

For a complex safe set, defining a safe set using a single FMBF may be inadequate for capturing intricate or multiple safety constraints. In this subsection, we introduce a composite safe set defined by N differentiable continuous functions $h_j(\cdot) : \mathbb{S} \rightarrow \mathbb{R}$ with $j = 1, \dots, N$ and $N \in \mathbb{N}_{>0}$. Then a composite safe set \mathbb{C}_s is defined as

$$\mathbb{C}_s = \bigcap_{j=1}^N \mathbb{C}_{s,j}, \quad \mathbb{C}_{s,j} = \{\mathbf{s} \in \mathbb{S} : h_j(\mathbf{s}) \geq 0\}, \quad \forall j = 1, \dots, N. \quad (9)$$

We extend the definition of trajectory safety, safe flow matching, and FMBF from the unified case to this composite framework, as detailed below.

Definition 6 (Composite Flow Matching Barrier Function). The function $\mathbf{h}(\cdot) = [h_j(\cdot)]_{j=1, \dots, N}$ is called a composite flow matching barrier function (CFMBF) if it satisfies the following conditions:

1. For all $i = 0, \dots, H$ and $t \in [0, 1)$, there exists $\mathbf{u}_t^i \in \mathbb{R}^{d_s}$ such that

$$\frac{dh_j(\mathbf{E}_i \mathcal{T}_t)}{d\mathbf{E}_i \mathcal{T}_t} \mathbf{E}_i \mathbf{v}_t^\theta(\boldsymbol{\tau}) + \frac{dh_j(\mathbf{E}_i \mathcal{T}_t)}{d\mathbf{E}_i \mathcal{T}_t} \mathbf{u}_t^i + \varphi_j(t, h_j(\mathbf{E}_i \mathcal{T}_t)) h_j(\mathbf{E}_i \mathcal{T}_t) \geq 0 \quad (10)$$

holds for all $j = 1, \dots, N$, where $\varphi_j(t, h_j(\mathbf{s})) = \varphi_{0,j}$ if $h_j(\mathbf{s}) \geq 0$ with $\varphi_{0,j} \in \mathbb{R}_{>0}$, and $\varphi_j(t, h_j(\mathbf{s})) = \varphi_{1,j}(t)$, otherwise. The blow-up function $\varphi_{1,j}(\cdot) : [0, 1) \rightarrow \mathbb{R}_{>0}$ monotonically increases satisfying $\lim_{t \rightarrow 1^-} \varphi_{1,j}(t) = +\infty$ and $\int_0^{1^-} \varphi_{1,j}(s) ds = \infty$.

2. For all $i = 0, \dots, H$ and $j = 1, \dots, N$, the terminal condition holds: $h_j(\mathbf{E}_i \mathcal{T}_1) \geq 0$.

³For the detailed proofs, refer to Appendix A.

Definition 7 (Trajectory Safety with CFMBF). A trajectory \mathcal{T} of length $H + 1$ is safe if satisfies the condition in Definition 3 w.r.t $h_j(\cdot)$ for all $j = 1, \dots, N$.

Definition 8 (Safe Flow Matching with CFMBF). A flow matching process is called safe w.r.t. composite $\mathbf{h}(\cdot)$, if the generated trajectory \mathcal{T}_1 at $t = 1$ is safe w.r.t. composite $\mathbf{h}(\cdot)$ defined by Definition 7 for any initial sample $\mathcal{T}_0 \sim p_0$.

Building on the safety guarantees established for a unified safe set, we demonstrate that a CFMBF ensures the safety of both the trajectory and the FM process in the composite case, as formalized below.

Theorem 2. Suppose $\mathbf{h}(\cdot)$ is a valid CFMBF as defined in Definition 6. Then, the flow matching process is safe according to Definition 8, and the trajectory \mathcal{T}_1 satisfies the safety conditions in Definition 7.

Same as the scenario in the unified contracts, we incorporate a minimal regularization term \mathbf{u}_t into the flow matching process while ensuring safety under composite constraints. For SafeFlow under composite constraints, the QP problem is formulated to determine \mathbf{u}_t for any $t \in [0, 1)$ as

$$\mathbf{u}_t = \underset{\mathbf{u}=[\mathbf{u}^{0^\top}, \dots, \mathbf{u}^{H^\top}]^\top \in \mathbb{R}^d}{\arg \min} \|\mathbf{u}\|^2 \quad (11a)$$

$$\text{s.t. } \frac{dh_j(\mathbf{E}_i \mathcal{T}_t)}{d\mathbf{E}_i \mathcal{T}_t} \mathbf{E}_i \mathbf{v}_i^\theta(\boldsymbol{\tau}) + \frac{dh_j(\mathbf{E}_i \mathcal{T}_t)}{d\mathbf{E}_i \mathcal{T}_t} \mathbf{u}^i + \varphi_j(t, h_j(\mathbf{E}_i \mathcal{T}_t)) h_j(\mathbf{E}_i \mathcal{T}_t) \geq 0, \quad (11b)$$

$$\forall i \in \{0, \dots, H\}, \forall j \in \{1, \dots, N\}.$$

5 Experimental Results

We conduct simulation experiments to answer the following questions:

- Q1:** Does SafeFlow generate obstacle-avoiding trajectories with provable safety guarantees?
- Q2:** What impact do FMBFs have on the diffusion and flow-based model in the inference process?
- Q3:** How does SafeFlow perform in comparison to SOTA methods that incorporate safety constraints?

In particular, we compare against several SOTA methods, including all variants of SafeDiffuser [22]: Robust-Safe Diffuser (RoSD), Relaxed-Safe Diffuser (ReSD), and Time-Varying-Safe Diffuser (TVSD), as well as CoB and CoBL from [23], which combine control barrier functions with or without Lyapunov functions within the diffusion framework. Besides the conventional guidance-based approaches, such as Classifier Guidance (CG) [29] and Truncate (TRUNC) [30], we implement our proposed FMBFs on top of the diffusion model, named SafeDiffus, to ensure safety guarantees.

5.1 Robot Navigation

In this subsection, we consider a simple task that the robot can navigate in planar directions from the lower-left to upper-right as illustrated in Fig. 2. This experiment evaluates the performance of SafeFlow and SafeDiffus and other methods for planar robot navigation with six metrics⁴.

- The safety rate (**Safety**) indicates the proportion of generated trajectories that avoid collisions with obstacles.
- The Kullback–Leibler (KL) divergence of goal state distributions (**KL-G**) is utilized to quantify the discrepancy between the generated data distribution and the true distribution observed in the dataset, which indicates the reachability of the generated final states.
- Moreover, we use curvature-based smoothness (**CS**) to quantify the smoothness of discrete trajectories, which captures the degree of directional change between consecutive path segments, and acceleration-based smoothness (**AS**) to assess the change in velocity.

⁴Additional details and results are provided in Appendix C.

- Inference time (**Time**) measured the duration required to generate a single trajectory.

To illustrate the effectiveness of SafeFlow in generating safe, smooth, and goal-directed trajectories for planar robot navigation, we qualitatively analyze the trajectory generation process based on benchmark experiments with 1000 trials in Table 1. Notably, SafeFlow achieves a perfect safety rate of 100%, significantly outperforming all baselines with safety guarantees, which provides both experimental and theoretical support for **Q1**. It is noted that the safety claimed in [23, 22] is only probabilistic due to the stochastic property of the diffusion model and the utilization of conventional CBF, which induces low safety in our scenarios. To answer **Q2**, we further analyze the differences between the vanilla FM and SafeFlow, as well as the vanilla Diffuser and SafeDiffus. SafeFlow and SafeDiffus incur approximately 60% higher inference time due to the safety regularization. Nevertheless, they outperform other baselines that incorporate safety strategies. The increases in KL-G and CS are expected, as the models need to make directional adjustments to avoid obstacles. Notably, the lower CS values of FM and the vanilla Diffuser reflect overly simplistic, straight-line trajectories that compromise safety. Interestingly, in the AS metric, our SafeDiffus outperforms the vanilla Diffuser, while FM and SafeFlow and FM yield the lowest AS scores. The answer to **Q3** is illustrated in Fig. 2, which visually compares the trajectory generation performance across different methods. It is evident that SafeFlow effectively avoids obstacles while closely adhering to the trajectory distribution observed in the training dataset. SafeDiffus also achieves zero collisions; however, some outliers remain, where a few generated trajectories exhibit higher sensitivity. In contrast, other approaches either collide with obstacles or generate trajectories that deviate significantly from the training distribution. This highlights the ability of the proposed framework to outperform SOTA methods, offering both training-free deployment and test-time safety guarantees.

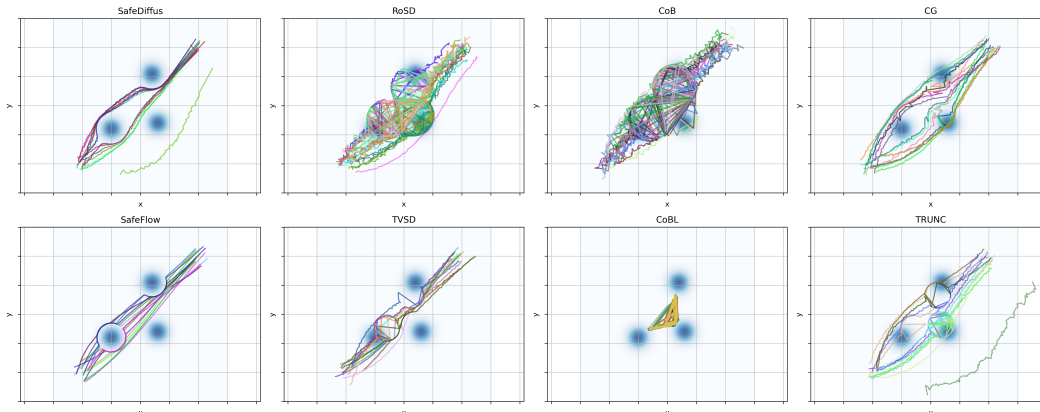


Figure 2: Comparison of generated trajectories from 15 samples across different methods.

Table 1: Safe planning for robot navigation comparisons with benchmarks.

Method	Safety \uparrow	KL-G \downarrow	CS \downarrow	AS \downarrow	Time (s) \downarrow
CG [29]	10.39%	0.0252	0.2492	0.0152	0.96
TRUNC [30]	11.24%	0.0254	0.4668	0.6131	0.93
RoSD [22]	5.42%	0.0303	0.4747	0.0837	29.84
TVSD [22]	15.51%	0.0241	0.3283	0.0311	27.62
ReSD [22]	9.38%	0.0257	0.0629	0.1068	32.54
CoB [23]	9.59%	0.0248	0.5548	0.6561	1.29
CoBL [23]	2.40%	$> 10^{16}$	0.5102	0.7294	4.32
Diffuser [2]	10.58%	0.0224	0.0522	0.2858	0.31
SafeDiffus (Ours)	100.00%	0.0233	0.0985	0.0589	0.54
FM [7]	10.96%	0.0265	0.0040	0.0001	0.26
SafeFlow (Ours)	100.00%	0.0291	0.1150	0.0062	0.38

5.2 Robot Manipulation

To demonstrate the effectiveness of the proposed SafeFlow and SafeDiffus methods, we evaluate the same metrics used in Section 5.1 for a robotic manipulation task using Franka Research 3as shown in Fig. 3a. Specifically, the objective is to move the robot arm from a lower to an upper position without collision with obstacles, which are unseen in the training data sets. The experiment is repeated 1000 times for each method, and the performance of each method is evaluated based on the metrics mentioned in Section 5.1 for the motion trajectory of the end-effector, which is summarized in Table 2. It is obvious to see that the proposed SafeFlow demonstrates clear superiority in KL-G, CS, and inference time (except vanilla diffusion and flow models), especially in the safety aspect with 100% safety guarantees, providing a strong affirmative to Q1. It is noted that some baseline methods (Diffuser, FM, and ReSD) have low CS or AS due to the generation of overly simplified trajectories, lacking the effective response to obstacles and inducing insecurity. Therefore, SafeFlow demonstrates better performance compared to the SOTA methods [22, 23, 29, 30] that integrate safe constraints, which answers Q3. A similar phenomenon observed in Section 5.1 is that there is a slight degradation in performance compared to vanilla approaches (Diffuser and FM) is expected, as the FMBFs influence the generation process during inference to enforce safety.

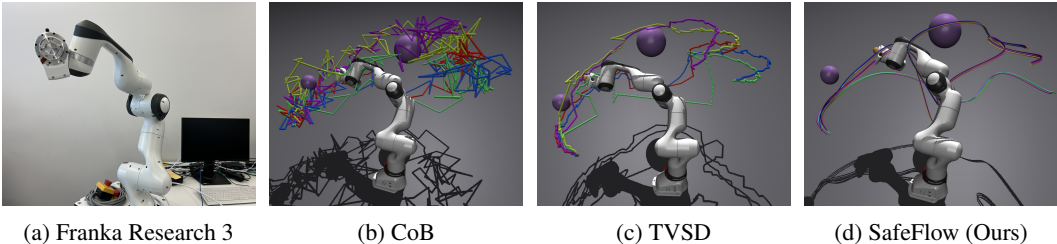


Figure 3: End-effector trajectories for selected methods. (a) Tested Franka Research 3. (b-c) Demonstration of end-effector trajectories from experiments, where (b,c) are chosen with the highest safety rate in [22, 23].

Table 2: Safe planning for robot manipulation comparisons with benchmarks.

Method	Safety \uparrow	KL-G \downarrow	CS \downarrow	AS \downarrow	Time \downarrow
CG [29]	27.63%	0.3221	0.6897	0.0223	20.02
TRUNC [30]	33.31%	0.1199	0.6734	0.0135	19.80
RoSD [22]	68.22%	0.2246	0.6168	0.0227	40.16
TVSD [22]	69.31%	0.1219	0.6855	0.0253	123.47
ReSD [22]	39.28%	0.1436	0.6729	0.0129	66.46
CoB [23]	34.51%	0.4257	0.6528	0.0345	20.16
CoBL [23]	23.21%	0.5668	0.6330	0.0497	20.29
Diffuser [2]	10.03%	0.0378	0.6207	0.0126	16.61
SafeDiffus (Ours)	100.00%	0.0711	0.6542	0.0408	41.65
FM [7]	13.98%	0.0227	0.1006	0.0196	5.13
SafeFlow (Ours)	100.00%	0.0612	0.1734	0.0251	14.76

6 Conclusion

In this paper, we tackled the critical challenge of enabling robots to generate safe and efficient trajectories in dynamic and unseen obstacles, a fundamental requirement for autonomous systems in real-world applications. Existing generative methods, such as diffusion models, while capable of modeling complex trajectory distributions, often incur high computational costs and lack explicit safety guarantees, limiting their practical applications in safety-critical scenarios. To address these shortcomings, we proposed SafeFlow, a novel motion planning framework that integrates flow matching with FMBFs inspired by CBFs. Our proposed SafeFlow ensures trajectory safety while maintaining computational efficiency. Specifically, SafeFlow leverages the deterministic and efficient nature of

flow matching to transform samples from a simple prior distribution into goal-directed trajectories, embedding safety constraints directly into the learned flow field via FMBFs. This approach guarantees that generated trajectories remain within safe regions throughout the planning horizon, even in the presence of unseen obstacles or dynamic constraints. Our experimental evaluations, including planar robot navigation and 7-DoF robot manipulation, demonstrated the superior performance of SafeFlow over SOTA planners. These advantages make it highly suitable for real-time safety-critical applications.

References

- [1] A. Sridhar, D. Shah, C. Glossop, and S. Levine. NoMaD: Goal Masked Diffusion Policies for Navigation and Exploration. In *2024 IEEE International Conference on Robotics and Automation (ICRA)*, pages 63–70, 2024. doi:10.1109/ICRA57147.2024.10610665.
- [2] M. Janner, Y. Du, J. Tenenbaum, and S. Levine. Planning with Diffusion for Flexible Behavior Synthesis. In *Proceedings of the 39th International Conference on Machine Learning*, volume 162 of *Proceedings of Machine Learning Research*, pages 9902–9915. PMLR, 17–23 Jul 2022. URL <https://proceedings.mlr.press/v162/janner22a.html>.
- [3] D. Gadginmath and F. Pasqualetti. Dynamics-aware Diffusion Models for Planning and Control, 2025. URL <https://arxiv.org/abs/2504.00236>.
- [4] Y. Song, J. Sohl-Dickstein, D. P. Kingma, A. Kumar, S. Ermon, and B. Poole. Score-Based Generative Modeling through Stochastic Differential Equations. In *International Conference on Learning Representations*, 2021. URL <https://openreview.net/forum?id=PxtTIG12RRHS>.
- [5] G. Zhou, S. Swaminathan, R. V. Raju, J. S. Guntupalli, W. Lehrach, J. Ortiz, A. Dedieu, M. Lázaro-Gredilla, and K. Murphy. Diffusion Model Predictive Control, 2024. URL <https://arxiv.org/abs/2410.05364>.
- [6] P. Glotfelter, J. Cortés, and M. Egerstedt. Nonsmooth Barrier Functions With Applications to Multi-Robot Systems. *IEEE Control Systems Letters*, 1(2):310–315, 2017. doi:10.1109/LCSYS.2017.2710943.
- [7] Y. Lipman, R. T. Q. Chen, H. Ben-Hamu, M. Nickel, and M. Le. Flow Matching for Generative Modeling. In *The Eleventh International Conference on Learning Representations*, 2023. URL <https://openreview.net/forum?id=PqvMRDCJT9t>.
- [8] N. Kornilov, P. Mokrov, A. Gasnikov, and A. Korotin. Optimal Flow Matching: Learning Straight Trajectories in Just One Step. In A. Globerson, L. Mackey, D. Belgrave, A. Fan, U. Paquet, J. Tomczak, and C. Zhang, editors, *Advances in Neural Information Processing Systems*, volume 37, pages 104180–104204. Curran Associates, Inc., 2024. URL https://proceedings.neurips.cc/paper_files/paper/2024/file/bc8f76d9caadd48f77025b1c889d2e2d-Paper-Conference.pdf.
- [9] X. Liu, C. Gong, and qiang liu. Flow Straight and Fast: Learning to Generate and Transfer Data with Rectified Flow. In *The Eleventh International Conference on Learning Representations*, 2023. URL <https://openreview.net/forum?id=XVjTT1nw5z>.
- [10] T. Xie, Y. Zhu, L. Yu, T. Yang, Z. Cheng, S. Zhang, X. Zhang, and C. Zhang. Reflected Flow Matching. In R. Salakhutdinov, Z. Kolter, K. Heller, A. Weller, N. Oliver, J. Scarlett, and F. Berkenkamp, editors, *Proceedings of the 41st International Conference on Machine Learning*, volume 235 of *Proceedings of Machine Learning Research*, pages 54614–54634. PMLR, 21–27 Jul 2024. URL <https://proceedings.mlr.press/v235/xie24k.html>.

- [11] J. Carvalho, A. T. Le, M. Baierl, D. Koert, and J. Peters. Motion Planning Diffusion: Learning and Planning of Robot Motions with Diffusion Models. In *2023 IEEE/RSJ International Conference on Intelligent Robots and Systems (IROS)*, pages 1916–1923, 2023. doi:10.1109/IROS55552.2023.10342382.
- [12] T. Pearce, T. Rashid, A. Kanervisto, D. Bignell, M. Sun, R. Georgescu, S. V. Macua, S. Z. Tan, I. Momennejad, K. Hofmann, and S. Devlin. Imitating Human Behaviour with Diffusion Models. In *The Eleventh International Conference on Learning Representations*, 2023. URL <https://openreview.net/forum?id=Pv1GPQzRrC8>.
- [13] M. Reuss, M. Li, X. Jia, and R. Lioutikov. Goal-Conditioned Imitation Learning using Score-based Diffusion Policies. In *Robotics: Science and Systems*, 2023.
- [14] Z. Xian, N. Gkanatsios, T. Gervet, T.-W. Ke, and K. Fragkiadaki. ChainedDiffuser: Unifying Trajectory Diffusion and Keypose Prediction for Robotic Manipulation. In *Proceedings of The 7th Conference on Robot Learning*, volume 229 of *Proceedings of Machine Learning Research*, pages 2323–2339. PMLR, 06–09 Nov 2023. URL <https://proceedings.mlr.press/v229/xian23a.html>.
- [15] W. Li, X. Wang, B. Jin, and H. Zha. Hierarchical Diffusion for Offline Decision Making. In *Proceedings of the 40th International Conference on Machine Learning*, volume 202 of *Proceedings of Machine Learning Research*, pages 20035–20064. PMLR, 23–29 Jul 2023. URL <https://proceedings.mlr.press/v202/li23ad.html>.
- [16] U. A. Mishra, S. Xue, Y. Chen, and D. Xu. Generative Skill Chaining: Long-Horizon Skill Planning with Diffusion Models. In *Proceedings of The 7th Conference on Robot Learning*, volume 229 of *Proceedings of Machine Learning Research*, pages 2905–2925. PMLR, 06–09 Nov 2023. URL <https://proceedings.mlr.press/v229/mishra23a.html>.
- [17] C. Chi, Z. Xu, S. Feng, E. Cousineau, Y. Du, B. Burchfiel, R. Tedrake, and S. Song. Diffusion policy: Visuomotor policy learning via action diffusion. *The International Journal of Robotics Research*, 0(0):02783649241273668, 2024. doi:10.1177/02783649241273668.
- [18] Y. Ze, G. Zhang, K. Zhang, C. Hu, M. Wang, and H. Xu. 3D Diffusion Policy: Generalizable Visuomotor Policy Learning via Simple 3D Representations. In *Proceedings of Robotics: Science and Systems (RSS)*, 2024.
- [19] H. Chen, J. Xu, L. Sheng, T. Ji, S. Liu, Y. Li, and K. Driggs-Campbell. Learning Coordinated Bimanual Manipulation Policies using State Diffusion and Inverse Dynamics Models, 2025. URL <https://arxiv.org/abs/2503.23271>.
- [20] A. Li, Z. Ding, A. B. Dieng, and R. Beeson. Constraint-Aware Diffusion Models for Trajectory Optimization, 2024. URL <https://arxiv.org/abs/2406.00990>.
- [21] J.-B. Bouvier, K. Ryu, K. Nagpal, Q. Liao, K. Sreenath, and N. Mehr. Ddat: Diffusion policies enforcing dynamically admissible robot trajectories, 2025. URL <https://arxiv.org/abs/2502.15043>.
- [22] W. Xiao, T.-H. Wang, C. Gan, R. Hasani, M. Lechner, and D. Rus. Safediffuser: Safe planning with diffusion probabilistic models. In *The Thirteenth International Conference on Learning Representations*, 2025. URL <https://openreview.net/forum?id=ig2wk7kK9J>.
- [23] K. Mizuta and K. Leung. CoBL-Diffusion: Diffusion-Based Conditional Robot Planning in Dynamic Environments Using Control Barrier and Lyapunov Functions. In *2024 IEEE/RSJ International Conference on Intelligent Robots and Systems (IROS)*, pages 13801–13808, 2024. doi:10.1109/IROS58592.2024.10802549.
- [24] F. Zhang and M. Gienger. Affordance-based Robot Manipulation with Flow Matching, 2025. URL <https://arxiv.org/abs/2409.01083>.

- [25] E. Chisari, N. Heppert, M. Argus, T. Welschehold, T. Brox, and A. Valada. Learning Robotic Manipulation Policies from Point Clouds with Conditional Flow Matching. In *8th Annual Conference on Robot Learning*, 2024. URL <https://openreview.net/forum?id=vtEn8NJWlz>.
- [26] Q. Zhang, Z. Liu, H. Fan, G. Liu, B. Zeng, and S. Liu. FlowPolicy: Enabling Fast and Robust 3D Flow-based Policy via Consistency Flow Matching for Robot Manipulation, 2024. URL <https://arxiv.org/abs/2412.04987>.
- [27] M. Braun, N. Jaquier, L. Rozo, and T. Asfour. Riemannian Flow Matching Policy for Robot Motion Learning. In *2024 IEEE/RSJ International Conference on Intelligent Robots and Systems (IROS)*, pages 5144–5151, 2024. doi:10.1109/IROS58592.2024.10801521.
- [28] I. Abel, D. Steeves, M. Krstić, and M. Janković. Prescribed-Time Safety Design for Strict-Feedback Nonlinear Systems. *IEEE Transactions on Automatic Control*, 69(3):1464–1479, 2024. doi:10.1109/TAC.2023.3326393.
- [29] P. Dhariwal and A. Nichol. Diffusion Models Beat GANs on Image Synthesis. In M. Ranzato, A. Beygelzimer, Y. Dauphin, P. Liang, and J. W. Vaughan, editors, *Advances in Neural Information Processing Systems*, volume 34, pages 8780–8794. Curran Associates, Inc., 2021. URL https://proceedings.neurips.cc/paper_files/paper/2021/file/49ad23d1ec9fa4bd8d77d02681df5cfa-Paper.pdf.
- [30] G. Brockman, V. Cheung, L. Pettersson, J. Schneider, J. Schulman, J. Tang, and W. Zaremba. OpenAI Gym, 2016. URL <https://arxiv.org/abs/1606.01540>.